Supplemental material for "The chemomechanics of crystallization during rewetting of limestone impregnated with sodium sulfate" by Rosa M Espinosa-Marzal, Andrea Hamilton, Megan McNall, Kathleen Whitaker, and George W. Scherer

1. Hygric expansion from swelling clays

To test the possibility that the measured expansion of CCL during water uptake results from swelling of clays, dilatation was measured in the DMA during imbibition of decane, which would not be expected to cause swelling of clays. A small swelling of CCL (5-12 μm/m) was observed, which leads to two different explanations for the measured hygric expansion:

- The Bangham effect (i.e. the reduction of the surface stress which leads to an expansion of the solid surface) might take place during adsorption of water vapor on the pore surface[1,2,3].

- A water meniscus that persists after drying might keep the sample in compression, which is released during the imbibition, yielding expansion.

The short time of exposure to ambient humidity before starting the measurement is not likely to have allowed significant adsorption of water vapor to take place, so the existence of a water meniscus after drying is the more likely explanation for the observed expansion. Due to the small magnitude of the swelling, it is difficult to determine the nature of the expansion; nevertheless, it must be taken into account for the analysis of the warping experiment.

2. Dilatation experiments using the Dynamic Mechanical Analyzer

The deformation of stone samples during drying-induced crystallization of sodium sulfate

salts was measured with a Dynamic Mechanical Analyzer (DMA 7e, Perkin Elmer). The goal of these experiments was to evaluate the stress induced in the stone by the crystallization of thenardite during the preliminary drying at 105 ºC. CCL samples (15 x 6 x 6 mm) were submerged in water at 60 ºC and then dried in the DMA furnace. The length change of the sample was measured as the sample dried during heating to 95 ºC; following an isothermal hold, the sample was cooled to 30 ºC. The same (dry) sample was then submerged in a 40 %w/w sodium sulfate solution (*viz*., the saturation concentration at 30 ºC) at 60 ºC for 1 hour and dried inside the DMA using the same temperature cycle. The pore filling by thenardite in the stone was 11.97 vol% at the end of the experiment. This pore filling is higher than in the samples used for the warping experiment (section 4.4) saturated with the same solution and dried at 105 ºC for several weeks (9.32 ± 0.75 vol%), suggesting that trapped water has remained in the DMA samples due to the short duration of the drying. That is, some of the pores are partially or completely blocked by salt, so that the solution is very slow to escape.

Figure A shows the measured strain of one CCL sample saturated with water and dried in the DMA (labeled as H_2O). The dotted line gives the strain of the same sample, but saturated with sodium sulfate solution (labeled as SS40). The strain passes through a maximum at 95 ºC and then partially relaxes as crystals grow on their unconfined surfaces (*i.e.*, the crystals consume the supersaturation by growing parallel to the pore wall). The final strain difference for a sample first saturated with water and then with solution is 120 ± 10 μm/m (obtained from 4 experiments) and it does not relax completely during the isothermal hold (there is only a small relaxation at 95 ºC), showing that the thenardite crystals exert a non-negligible crystallization pressure. There are two possible explanations for this. There might be a residual film of confined solution that becomes discontinuous by severe drying, whose supersaturation is responsible for

the constant crystallization pressure. (See Figure 8 in ref. 4) This is supported by the incomplete drying of the samples in the DMA. On the other hand, a constant strain might be caused if the crystallization pressure reached the disjoining pressure during the drying (*i.e.*, the maximal crystallization pressure), causing the crystals to come into direct contact with the pore wall, thereby stopping the growth. In that case, the crystals would also remain under pressure, which would be equal to the disjoining pressure. From our experimental results we cannot distinguish between these possibilities.

Although the measured strain difference at the highest thenardite content (~120 μm/m) is smaller than the failure strain of CCL (see table 1), the distribution of thenardite is most probably non-uniform (see section 3.2) and therefore higher local deformations and local damage cannot be excluded during the drying-induced crystallization of thenardite.

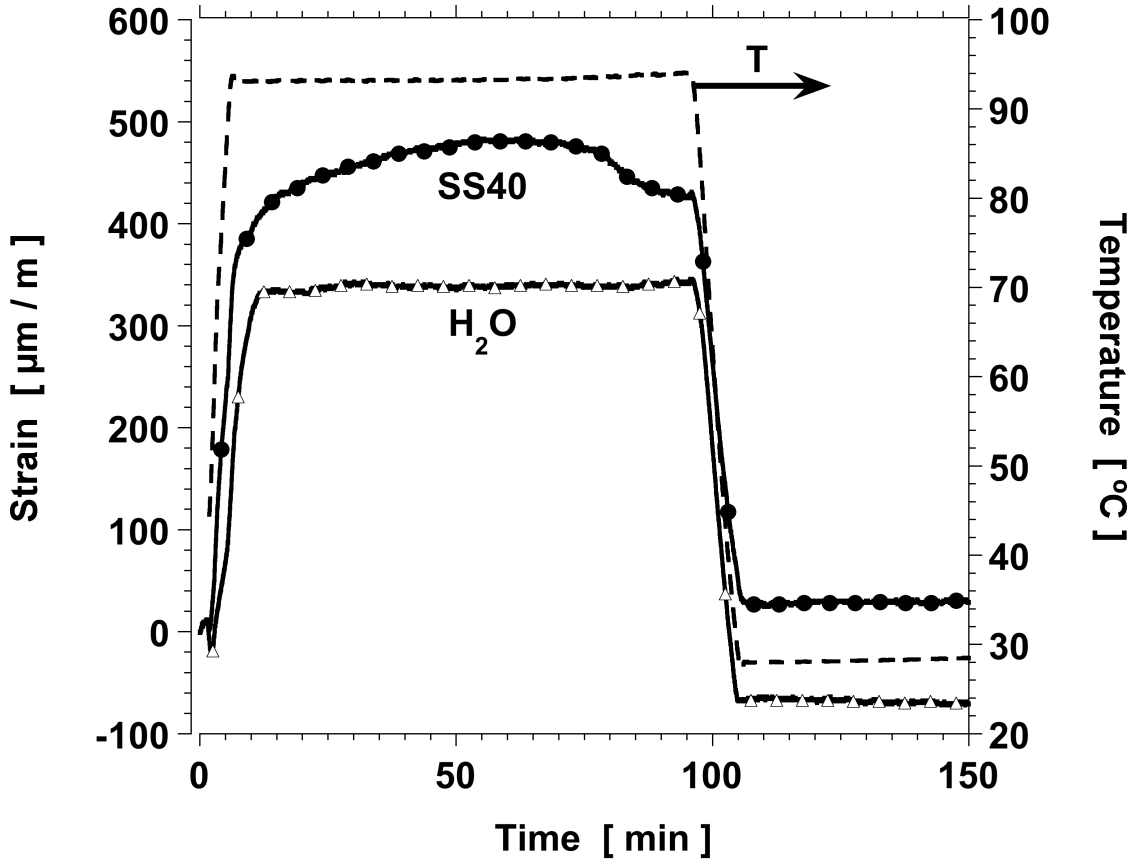

Figure A. Strain measured by DMA during the drying of a CCL sample first saturated at 60 ˚C with water (H_2O) and during the drying of the same sample saturated with sodium sulfate solution 40 %w/w (SS40). The drying period at 95 ˚C is followed by cooling to 30 ˚C. The temperature cycles of the two experiments are indistinguishable in the diagram.

3. Solution of the bending problem

The general linear elastic solution of the bending problem can be found in ref. 5. We define the free strain ε_f as the linear strain that the stone would exhibit if it were not constrained by the glass. We use the relation between the curvature due to bending w_{xx} and the free strain ε_f

given by:

$$w_{xx} = \frac{f_1 g_0 - f_0 g_1}{g_1^2 - g_0 g_2} \tag{1}$$

with

$$f_n = \int_{-h/2}^{h/2} \left(\frac{E\varepsilon_f}{1-\nu_s} \right) z^n dz \tag{2}$$

and

$$g_n = \int_{-h/2}^{h/2} \left(\frac{E}{1-\nu} \right) z^n dz \tag{3}$$

where z is the position along the thickness (see Figure 1 of the text), ε_f the free strain as a function of z, w_{xx} the curvature due to the bending (in 1/m), E the Young modulus of the material at location z, ν the Poisson ratio of the material at location z and h the thickness of the glass-stone composite glued with epoxy. This solution is applied to the particular case of a tri-material strip, allowing for differences in the elastic properties and free strain in each material (E_s, ν_s for the stone, E_{epx}, ν_{epx} for the epoxy layer and E_g, ν_g for the glass, see Fig. B). The measured deflection Δ_{exp} is related to the curvature w_{xx} by:

$$w_{xx} = -\frac{8\Delta_{\text{exp}}}{L^2} \tag{4}$$

where L is the length of the span of the composite (*i.e.,* the distance between the supports).

It has been shown that the initial *zero* deflection corresponds to a stressed state of the stone owing to thenardite crystallized during drying. The superposition of the contraction during

thenardite dissolution (positive deflection) and the expansion during mirabilite crystallization (negative deflection) leads to the measured deflection. To determine the absolute deflection owing to mirabilite exerting pressure on the pore wall, it is necessary to determine the "unstressed" reference state, which is reached after the complete dissolution of thenardite. Since there is no certainty about when this happens, the reference state is assumed to be the point of maximal positive deflection in the measurement. The difference between the measured deflection and the reference deflection is used to determine the curvature w_{xx} with eq. (4).

Given a known salt distribution, the integrals f_n and g_n can be evaluated analytically. We assume that the free strain ε_f is *uniform* (and non-zero) within the crystallization front, so

$$f_n = \int_{z_{s,1}}^{z_{s,2}} \frac{E_s^* \varepsilon_f}{1-\nu^*} z^n dz \tag{5}$$

and

$$\begin{aligned} g_n = & \int_{-h/2}^{z_{s,1}} \left(\frac{E_s}{1-\nu_s} \right) z^n dz + \int_{z_{s,1}}^{z_{s,2}} \left(\frac{E_s^*}{1-\nu^*} \right) z^n dz + \int_{z_{s,2}}^{LI} \left(\frac{E_s}{1-\nu_s} \right) z^n dz \\ & + \int_{LI}^{LI+d_{Epx}} \left(\frac{E_{Epx}}{1-\nu_{Epx}} \right) z^n dz + \int_{LI+d_{Epx}}^{h/2} \left(\frac{E_g}{1-\nu_g} \right) z^n dz \end{aligned} \tag{6}$$

where LI is the position of the glass-stone interface (in m), $z_{s,1}$ the start of the crystallization front (close to the wet surface) (in m), $z_{s,2}$ the end of the crystallization front (in m), d_{Epx} the thickness of the epoxy layer (in m), E^*_s the Young modulus of stone with salt in the pores and ν^* the Poisson ratio of stone with salt in the pores. Thus, Young's modulus of stone with salt in the pores (E^*_s) has to be considered only in $z_{s,1} < z < z_{s,2}$ as a function of the salt content. The influence of salt on Poisson's ratio is neglected ($\nu^* \sim \nu_s$).

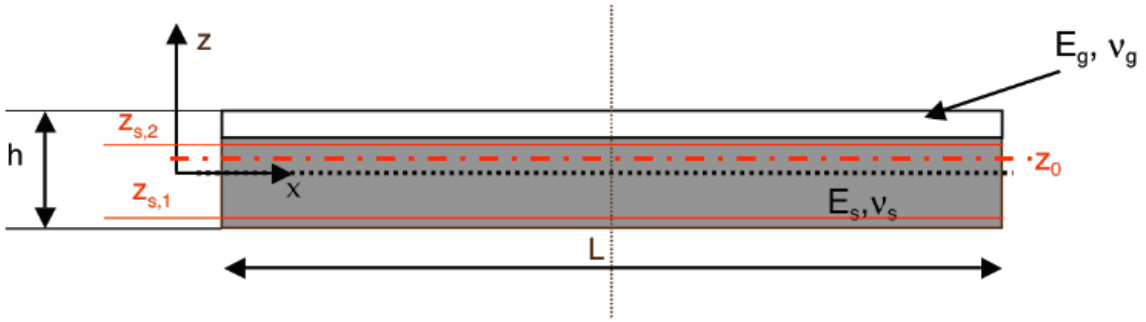

Figure B. Schematic of the glass-stone composite with length L = 100 mm, thickness $h \approx 13$ mm. The midplane ($z = 0$) is situated at $h/2$ and the neutral axis for bending at z_0. Crystallization occurs between $z_{s,1}$ and $z_{s,2}$. The liquid is in contact with the bottom of the stone plate (with properties E_s and ν_s) and the glass plate (properties E_g and ν_g) is on top.

The change in Young's modulus with salt content $E_s^{*\pm}$ can be estimated with the maximal (or minimal) bounds for the bulk modulus $K_s^{*\pm}$ and shear modulus $G_s^{*\pm}$ according to Hashin[6]. Hashin also describes how to determine the general bounds $K_s^{*\pm}$ and $G_s^{*\pm}$ for an isotropic particulate composite with more than 2 components as a function of the component volume fractions and their corresponding bulk and shear moduli. In our case, the system consists of matrix (*i.e.*, nonporous stone), solution, salt crystals, and air; the bulk and shear contributions of air and solution are negligible. The following data were used to estimate the bounds of the mechanical properties of the salt-bearing stone. The bulk and shear moduli of the thenardite crystals are K_c = 43.4 GPa and G_c = 22.3 GPa, respectively [7], which means that E_c = 57.1 GPa and ν_c = 0.28. For mirabilite we estimate a bulk modulus of $K_c \approx 22$ GPa by comparison with other highly hydrated salts for which the bulk modulus is known. For example, epsomite ($MgSO_4.7H_2O$) and ikaite ($CaCO_3.6H_2O$) have bulk moduli of 21.3 and 21.5 GPa respectively[8,9] and assuming ν_c = 0.28 (which is the Poisson's ratio of thenardite), the shear modulus of

mirabilite is $G_c \approx 11$ GPa. For the matrix of IL (non-porous calcite), Hart and Wang[10] determined experimentally the bulk modulus K_m = 72.6 GPa. According to Mavko *et al*., [11] the shear modulus of calcite is $G_m = 30.2 \pm 1.8$ GPa.

The measured Young's moduli of the salt-free and thenardite-bearing stones (see section 4.1 of the text) are not well described by either of the bounds estimated with Hashin's model, presumably because the cementing is not as stiff as the grains, but they fall well within the estimated bounds. Therefore, we used this model to predict the linear *change* of Young's modulus with the amount of mirabilite $E^{*+}{}_s$ reaching a maximal increase of 19.8 % for CCL and 16.8 % for IL at a degree of pore-filling of 100%, and assuming elastic behavior (and therefore excluding damage).

The analytical solution of the mechanical problem, eqs. (1)-(6), is evaluated with the only assumption being that the deformation ε_f within the crystallization front is uniform. Firstly, the curvature w_{xx} is computed with eq. (4) from the measured deflection. If the distribution of mirabilite in the stone plates during the warping experiment is known, the free strain ε_f can be determined with eq. (1) together with f_n and g_n defined in eqs. (5) and (6), respectively.

We assume an energy criterion that predicts failure when the strain energy imposed by the in-pore crystallization pressure:

$$W_c = \frac{\sigma^{*2}}{2K} \tag{7}$$

exceeds the failure strain energy obtained in a uniaxial tensile strength test, which is given by:

$$W_u = \frac{\sigma_T^2}{2E} \tag{8}$$

If the failure criterion is $W_c \geq W_u$, then failure is expected when

$$3(1-2\nu)\sigma^{*2} \geq \sigma_T^2 \tag{9}$$

We made a numerical assessment of the distribution of mirabilite in the warping plates during rewetting of thenardite with the reactive transport model, ASTra [12]. The rewetting process is governed by the advective transport of the solution or water through the pores and the kinetics of dissolution of thenardite and crystallization of mirabilite.

The permeability of a porous material is influenced by the crystals precipitated in the pores (*i.e.*, by pore clogging). At pore-filling ratios smaller than 5%, the effect of the reduced porosity on the capillary uptake is negligible. However, at larger salt contents and/or when mirabilite precipitates, pore clogging becomes more effective at reducing the permeability. To account for the influence of crystals in the pores, the pore size distribution is modified by assuming the volume occupied by mirabilite crystals during rewetting is uniform throughout all pore sizes and reduces the pore space. By applying Mualem's model,[13] the permeability can be expressed as a function of the reduced porosity at a given salt content. In this way, the influence of the precipitated salt on the capillary transport is considered in the numerical simulation of the rewetting process.

The kinetics of thenardite dissolution and mirabilite crystallization are estimated as a function of the supersaturation ratio, β. According to Nielsen[14] and Espinosa *et al.* [15] kinetic laws of the following type can be used for the rates of crystallization and dissolution of salts in porous materials:

$$\frac{dn_c}{dt} = K_{cr} \cdot (\beta - 1)^{g_{cr}} > 0 \tag{10}$$

and

$$\frac{dn_c}{dt} = -K_{dis} \cdot (1 - \beta)^{g_{dis}} < 0 \tag{11}$$

where K_{cr}, g_{cr} are the kinetic constants for crystallization, and K_{dis}, g_{dis} for dissolution, n_c the amount of precipitated salt and t the time.

A parametric study using the numerical model indicates that the dissolution rate of thenardite and the crystallization of mirabilite strongly influence each other, as well as the final distribution of mirabilite in the sample. Thus, slow dissolution of thenardite retards the crystallization of mirabilite, since the supersaturation with respect to mirabilite is smaller, while rapid dissolution of thenardite maintains the concentration equal to the solubility of thenardite. On the other hand, fast crystallization of mirabilite accelerates the dissolution of thenardite, since the solution quickly becomes significantly under-saturated with respect to thenardite. So far it has not been possible to determine the limiting step for the overall transformation in a pore experimentally. Hence, the rate of the dissolution-crystallization reaction given by eqs. (13) and (14) was fitted to the results of the synchrotron analysis shown in Figure 3 of the text.

References

1. G.W. Scherer: Dilatation of Porous Glass. J. Am. Ceram. Soc. 69, 473 (1986).

2. M. Vandamme, L. Brochard, B. Lecampion and O. Coussy: Adsorption and Strain: The CO2-Induced Swelling of Coal, JMPS (2010).

3. J. Weissmuller and J.W. Cahn: Mean stresses in microstructures due to interface stresses: a generalization of a capillary equation for solids. Acta mater. 45, 1899 (1997)

4. G.W. Scherer: Stress from crystallization of salt , Cement Concr. Res. 34, 1613-1624 (2004).

5. G.W. Scherer: Drying gels. III Warping plate. J. Non-Cryst. Solids 9, 83 (1987).

6. Z. Hashin: Analysis of composite materials - A Survey. J. Appl. Mech. 50, 481 (1983).

7. C.J. Haecker, E.J. Garboczi, J.W. Bullard, R.B. Bohn, Z. Sun, S.P. Shah and T. Voigt: Modeling the linear elastic properties of Portland cement paste. Cem. Concr. Res. 35, 1948 (2005).

8. A.D. Fortes, I.G. Wood and K.S. Knight, J.P. Brodholt, M. Alfredsson and L. Vocadlo: Neutron diffraction studies of planetary ices. Lunar and Planetary Science XXXV (2004).

9. A.R. Lennie: Ikaite (CaCO3.6H2O) compressibility at high water pressure: A synchrotron X-ray diffraction study. Min. Mag. 69, 325 (2005).

10. D.J. Hart and H.F. Wang: Laboratory measurements of a complete set of poroelastic moduli for Berea sandstone and Indiana limestone. J. Geophys. Res. 100, 17741 (1995).

11. G. Mavko, T. Mukerji and J. Dvorkin: The Rock Physics Handbook: Tools for Seismic Analysis in Porous Media, Cambridge University Press, Cambridge (1998).

12. L. Franke, J. Kiekbusch, R. Espinosa and C. Gunstmann: CESA AND ASTRA – two program systems for cement and salt chemistry and the prediction of corrosion processes in concrete. Proceedings of International Conference on Durability of HPC and Final Workshop of CONLIFE, M. J. Setzer und S. Palecki, 501-508, Aedificatio Publishers, Essen (2007).

13. Y. Mualem: A new model for predicting the hydraulic conductivity of unsaturated porous media. Water resour. Res. 12, 513 (1976).

14. A.E. Nielsen: Electrolyte Crystal growth mechanisms. J. Cryst. Growth 67, 289 (1984).

15. R.M. Espinosa, L. Franke and G. Deckelmann: Phase changes of salts in porous materials. J.

Constr. Build. Mat. 22, 1758 (2007a).